Optics Communications 285 (2016) 2769–2773

Contents lists available at SciVerse ScienceDirect

Optics Communications

journal homepage: www.elsevier.com/locate/optcom

Minimum tangential error ophthalmic lens design without multi-parametric optimization

Sergio Barbero

Instituto de Optica (CSIC), Serrano 121, Madrid 28006, Spain

ARTICLE INFO

Article history:
Received 13 September 2011
Accepted 30 January 2012
Available online 14 February 2012

Keywords:
Ophthalmic lens design
Ophthalmic lenses
Optical design

ABSTRACT

Conventional ophthalmic lens design is based on minimizing a merit function with the help of optimization algorithms. As an alternative to this design strategy, I present a novel procedure for ophthalmic lens design, which main feature is that geometrical properties of the lens surface – specifically sag, surface normals, and surface curvatures – are constructed point-by-point. To show the potentials of the procedure, I present some design examples of positive and negative lenses where the tangential power error is virtually eliminated for all gaze directions (up to 40°).

1. Introduction

Besides mechanical, manufacturing and aesthetic constraints, the shape of ophthalmic lens surfaces is designed aim at improving the optical quality, for different gaze directions, by means of minimizing some optical aberrations. The monochromatic aberrations that are normally considered are oblique astigmatism and curvature of field (also called mean power error) [1], though the relevance of distortion has also been stressed [2]. Recently, even some authors start to contemplate other higher order aberrations [3].

However, to control these aberrations, ophthalmic lens design is limited by the few available degrees of freedom. Aspherical surfaces were introduced, among other reasons, to increase the number of design parameters. The first aspheric lenses with convex surfaces appeared at the end of the 1970's [4]. The majority of aspheric lenses are made aspheric on the front surface [5].

A fundamental question arises: given a single aspheric surface, which is the best strategy to maximize the optical quality? Following Schultz terminology [6], ophthalmic lens design can be considered as a case of *large fields imaging with thin pencils*. Schultz showed that, in general, such a system needs three aspheric surfaces to completely correct distortion, field of curvature and astigmatism [6]. Within this fundamental constraint, in ophthalmic lens design several partial correcting strategies have been proposed; two of the most popular ones are the point focal and Percival designs that correct the oblique astigmatism and mean power error respectively [4]. Nowadays, a typical strategy is to minimize the tangential power error. It has the advantage that if the real vertex distance is different from the value used in the design, the lens tends to behave as a point focal design (overestimation of the vertex distance) or as Percival design (subestimation of the vertex distance) [4]. In this work, I follow this approach.

The usual strategy in ophthalmic lens design is multi-parametric optimization. The method is based on searching for the coefficients of an analytical description of the lens surface which minimize a previously established merit function. This is performed with optimization algorithms. This procedure has the inherent problem of needing sophisticated optimization software, normally implemented in commercial optical design programs. In addition, as pointed out by Sun et al. [7], some special care must be taken to prevent problems such as the generation of surface profiles that are difficult to manufacture, e.g. with inflection points (zero second derivative). The new design procedure, that I present in this paper, constructs the surface smoothly point-by-point, so preventing such problems.

Not many authors have proposed optical design algorithms for large field systems without using multi-parametric optimization. Schultz [6] proposed a step-by-step surface construction algorithm to be used for systems containing four surfaces. A different algorithm, based on applying Fermats principle and the so-called pupil astigmatism criteria [8], has been recently proposed, also to be used for three or four surface systems [9]. In the field of illumination optics, the so-called Simultaneous-Multiple-Surface (SMS) method [10] ensures perfect imaging of coupled pair of wavefronts with two or more surfaces. Inspired by these strategies, the I present a novel non-optimization design algorithm to design ophthalmic single-vision lenses with one aspheric surface. The algorithm designs the front lens surface though it could be easily adapted to design the back surface of the lens.

E-mail address: sergio.barbero@csic.es.

0030-4018/$ – see front matter © 2012 Elsevier B.V. All rights reserved.
doi:10.1016/j.optcom.2012.01.071

2. Design procedure

2.1. Design scheme

Fig. 1 shows the scheme used in ophthalmic lens design. The center of rotation of the eye is located at point C. It is usually assumed that the distance from the spectacles back vertex to the center of rotation of the eye is 27 mm [1]. The sphere centered at C which radius of curvature is the aforementioned distance is called the vertex sphere.

In a backwards ray tracing, θ is the angle between the line set by the gaze direction and the optical axis of the eye-lens system. The intersection of the ray back-traced along the gaze direction with the vertex sphere is denoted by V. O is the intersection of this ray, after propagation inside the lens, with the anterior surface of the lens.

To compute the optical performance of the lens, a localized plane wavefront at point O is propagated till point V. From the principal curvatures of the wavefront at V the oblique astigmatism and power errors can be computed. Therefore, the design goal consists of setting these principal curvatures at point V.

2.2. Theoretical considerations

Before describing the design algorithm some theoretical issues must be explained. The algorithm is based on back and forward tracing of localized wavefronts. If the geometry of the lens surfaces is known, well established formulae have been derived to propagate localized wavefront through the lenses [11–14]. In the design procedure, the geometry of the surfaces are the unknown, but, as it will be shown in the next section, the refracted and the incident ray directions and wavefronts curvatures are known. As a consequence, the refraction formulae have to be rewritten.

Using the auxiliary function: $\mu = \sqrt{1+\beta^2-2\beta\left(\bar{r}-\bar{i}\right)}$ (β is the ratio between refractive indexes at each side of the surface) it is simple to derive the equation for the surface normal vector ($\bar{n}$) knowing the incident ($\bar{i}$) and the refracted ($\bar{r}$) ray vectors [15]:

$$\bar{n} = \frac{\bar{r}-\beta\bar{i}}{\mu}. \tag{1}$$

We confine our algorithm to design rotationally symmetric lenses. The meridians and parallels of any surface of revolution are lines of curvature [16]. The principal curvatures along the meridians and parallels are called tangential and sagittal curvatures respectively. Therefore, it is convenient to represent the lens surfaces explicitly in cylindrical coordinates; the sag coordinate (z) is given as a function of the radial (ρ) and azimuthal ϕ coordinates, so as the second partial derivative of z with respect to the radial coordinate can be calculated from the tangential curvature using the following equation:

$$\frac{\partial^2 z}{\partial \rho^2} = K_t\left(1+\left(\frac{\partial z}{\partial \rho}\right)^2\right)^{3/2}. \tag{2}$$

where K_t is the tangential curvature.

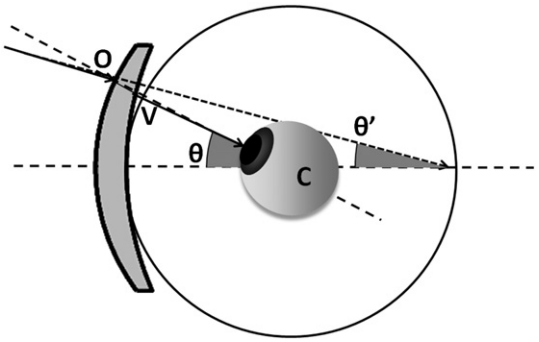

Fig. 1. General scheme to compute optical properties for different gaze directions. C is the center of rotation of the eye. V is the vertex sphere.

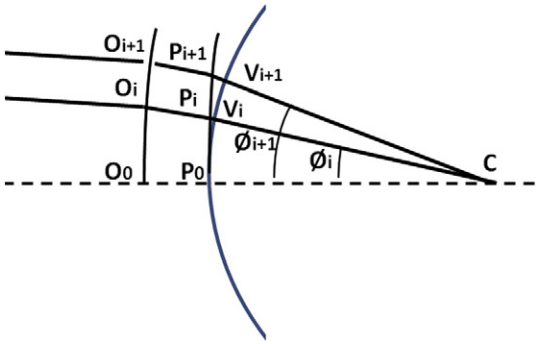

Fig. 2. Illustration of the design algorithm. C is the center of rotation of the eye. P_0 and O_0 are the back and front lens vertex points respectively. P_i and O_i denote points in the back and front lens surface respectively. V_i denote points i the vertex sphere.

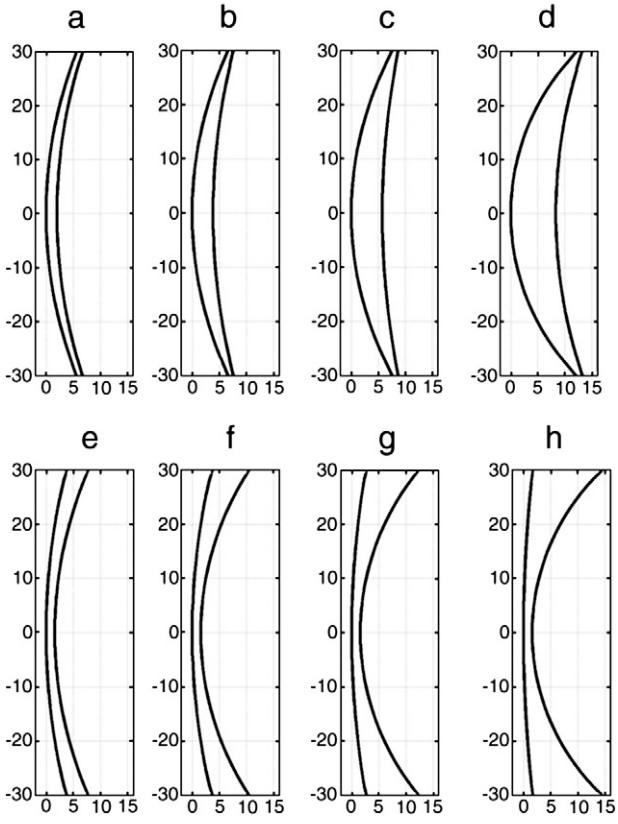

Fig. 3. Surface profiles of the lenses designed with the new procedure. Positive lenses: (a) 1 D (b) 3 D (c) 5 D (d) 7 D. Negative lenses: (e) −2.5 D (f) −5 D (g) −7.5 D (h) −10 D.

Table 1
Design specifications of the aspheric lenses. CT and ET denote central and edge thicknesses (mm) respectively. Ra and Rp are the radii of curvature of the anterior and posterior lens respectively. Qa is the conic parameter of the anterior surface and K_i are the high order coefficients of the anterior surface.

	1 D	3 D	5 D	7 D	−2.5 D	−5 D	−7.5 D	−10 D
CT	2	3.85	5.75	8.35	1.6	1.6	1.6	1.6
ET	1.107	1.099	1.163	1.13	3.954	6.719	9.571	12.67
Rp	98.644	120.632	153.069	94.181	76.413	55.228	47.385	41.485
Ra	82.932	70.993	62.058	43.172	124.807	125.052	167.264	252.054
Qa	0.0022	−6.24E−6	−0.0012	5.58E−4	−1.71E−4	6.1E−4	2.79E−4	−1.87E−4
K_1	7.32E−8	1.61E−7	2.03E−7	5.52E−7	−7.41E−8	−3.386E−7	−4.81E−7	−5.31E−7
K_2	−4.92E−10	−1.32E−9	−2.01E−9	−2.79E−9	9.04E−10	1.69E−9	2.07E−9	2.1E−9
K_3	1.99E−12	4.89E−12	6.83E−12	9.33E−12	−3.7E−12	−6.68E−12	−7.86E−12	−7.58E−12
K_4	−4.47E−15	−1.03E−14	−1.35E−14	−1.81E−14	8.23E−15	1.48E−14	1.69E−14	1.58E−14
K_5	5.35E−18	1.15E−17	1.42E−17	1.88E−17	−9.66E−18	−1.74E−17	−1.93E−17	−1.74E−17
K_6	−2.63E−21	−5.29E−21	−6.15E−21	−8.05E−21	4.65E−21	8.39E−21	9.04E−21	7.87E−21

Finally, to obtain the surface principal curvatures from the curvatures of the incident and refracted wavefront, I used the following equation derived from reference [14]:

$$\tilde{K} = \tilde{R}(\theta_s)^{-1}\frac{\tilde{L_1} - \tilde{R}(\varphi_1,\theta_1)\tilde{L_0}\tilde{R}(\varphi_1,\theta_1)^{-1}}{n_2 cos(\varphi_2) - n_1 cos(\varphi_1)}\tilde{R}(\theta_s). \quad (3)$$

where $\tilde{K}$ is the surface curvature matrix. The rest of the variables are explained at reference [14].

2.3. Design algorithm

The geometry of the algorithm is shown in Fig. 2.

The posterior lens surface is set to be a spherical surface. The algorithm starts from a paraxial pre-design. This means that the central thickness, points P_0 and O_0 in Fig. 2, and the apical curvatures at P_0 and O_0 are set. They are denoted by $K(P_0)$ and $K(O_0)$, respectively. As an example, these initial values could be obtained from the best-form Tscherning solution [5].

Exploiting the rotationally symmetry of the lens, only rays in a fixed meridian ($\phi = 0$) were considered. A ray is back-traced from point C having an angle θ_0 with the optical axis. Knowing that the posterior lens surface is spherical, it is straightforward to compute the intersection point of this ray with the posterior surface: P_1. The surface normal can be also computed at P_1, so refraction is applied at P_1.

The next step is to estimate the intersection point O_1 of this ray with the lens anterior surface. If θ_0 is selected to be sufficiently small, it is reasonable to assume that the anterior surface of the lens, in the neighborhood of O_0, contains O_1 and can be described with a sphere of curvature: $K(O_0)$. Now, it is straightforward to compute the coordinates of O_1 (intersection of a line with a circle).

From these initial values, a recurrence algorithm is established to construct the posterior surface by means of a set of points O_i, with its first and second derivatives with respect to ρ.

The construction works as follows. Let say that the point O_i, with coordinates $\{\rho_i, z_i\}$ and its first and second derivatives have been generated. A new ray is traced from point C having an angle $\theta_{i+1} = \theta_i + \varepsilon$,

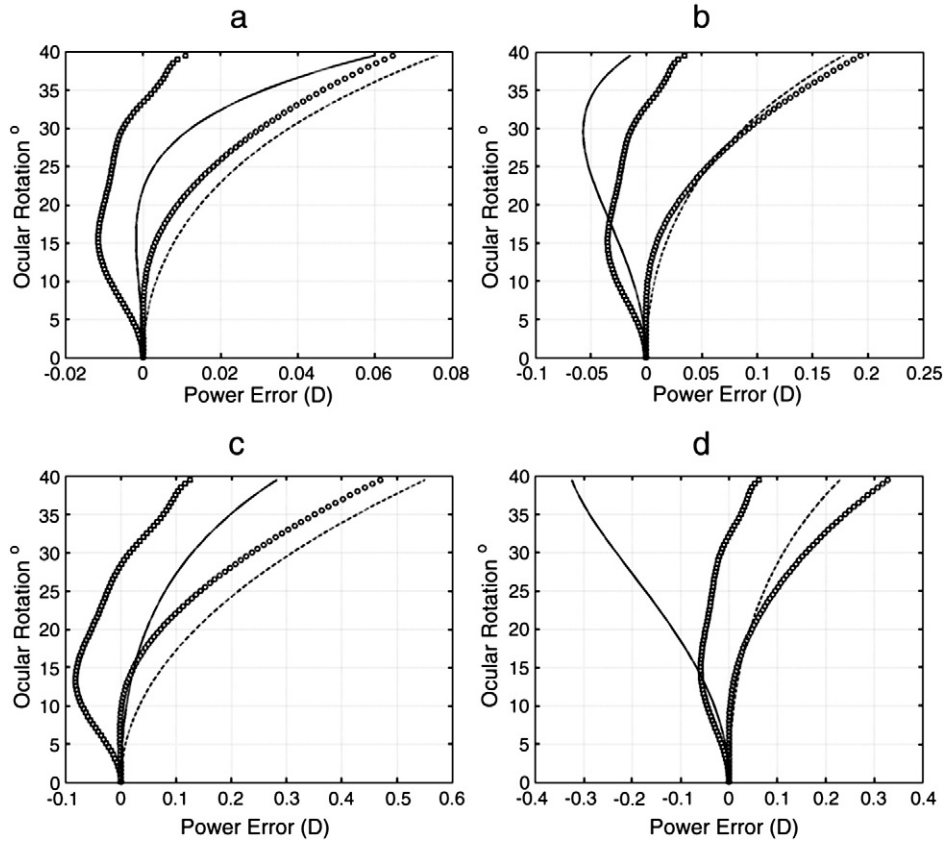

Fig. 4. Tangential and sagittal power error (D) as a function of ocular rotation (degrees) for the positive lenses: (a) 1 D (b) 3 D (c) 5 D (d) 7 D. Tangential and sagittal power error for the spherical lenses are plotted with solid and dashed lines respectively. Tangential and sagittal power error for the new aspheric lenses are plotted with squares and circles respectively.

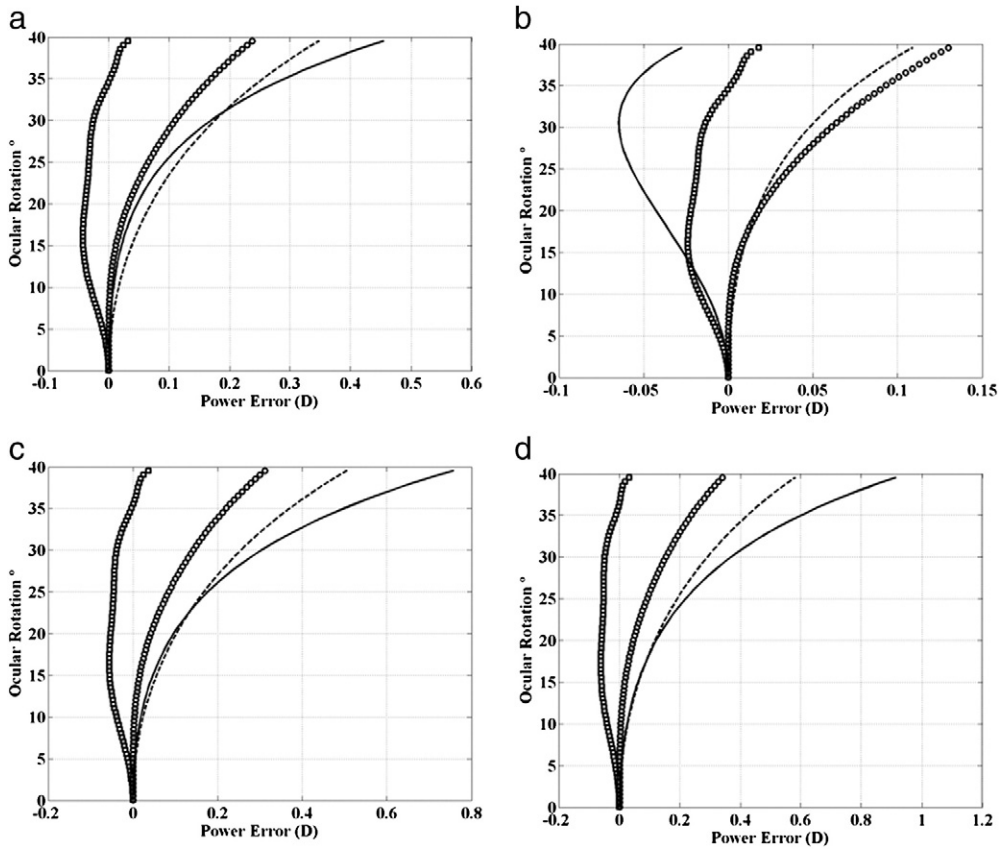

Fig. 5. Tangential and sagittal power error (D) as a function of ocular rotation (degrees) for the negative lenses: (a) −2.5 D (b) −5 D (c) −7.5 D (d) −10 D. Tangential and sagittal power error for the spherical lenses are plotted with solid and dashed lines respectively. Tangential and sagittal power error for the new aspheric lenses are plotted with squares and circles respectively.

being ε an arbitrarily small quantity. The intersection point at the posterior lens surface P_i+1, with its first and second derivatives are easily computed. Now, the anterior lens surface is locally described by a *quadratic patch* centered at O_i and described by the following equation:

$$z_{i+1}-z_i=\frac{\partial z_i}{\partial \rho}(\rho_{i+1}-\rho_i)+0.5\frac{\partial^2 z_i}{\partial \rho^2}(\rho_{i+1}-\rho_i)^2. \quad (4)$$

The coordinates (ρ_{i+1}, z_{i+1}) of the intersection point of the ray with this quadratic patch are found by solving the associated equations. Obviously $\phi_{i+1}=\phi_i=0$, because the rays are always contained in the fixed meridional plane.

The next step is to compute the principal surface curvatures at point O_{i+1} (as already mentioned, these are the tangential and sagittal curvatures for rotationally symmetric spectacles). In a forward ray tracing a plane wavefront incident onto O_{i+1}, and after propagation through the lens, intersects the vertex sphere at point V_{i+1}. The spectacle lens is free from mean oblique error and astigmatism at V_{i+1} if the localized wavefront at this point is a sphere with radius of curvature the back focal length of the lens. Now, this spherical wavefront is propagated backwards to the point P_{i+1} previously obtained. At P_{i+1} the wavefront is refracted, and later propagated till point O_{i+1}. So at point O_{i+1} we have the vergence matrix of the incident wavefront but also that of the refracted (plane incident wavefront in the forward ray tracing). Finally the tangential curvature is obtained using Eq. (3), and from it the second derivative using Eq. (2).

To move to the next iteration the algorithm still needs to calculate $\frac{\partial z_{i+1}}{\partial \rho}$ (used in Eq. (4)). However there are two ways to do this. The first derivative at the anterior surface could be set to impose distortion correction. Distortion is corrected if the magnification is the same for any gaze direction, so $\frac{tan(\theta_i)}{tan(\theta'_i)}=cte$ (see Fig. 1). Setting this condition implies that the surface normal at P_{i+1} is given by Eq. (1). However, as mentioned in the Introduction, a single surface is not sufficient to simultaneously correct one curvature aberration and distortion; this means that, in general, it is not possible to find a surface satisfying the curvature and surface normals obtained in this way.

Alternatively, in the algorithm, the first radial derivative at P_{i+1} was computed so it ensures certain continuity and smoothness in the lens surface. This is realized using the finite differences formula:

$$\frac{\partial z_{i+1}}{\partial \rho}=\frac{\partial z_i}{\partial \rho}+(\rho_{i+1}-\rho_i)\frac{\partial^2 z_i}{\partial \rho^2}. \quad (5)$$

2.4. Surface fitting

The designed surface is obtained as a set of points, with its first and second derivatives. The final step in the algorithm is to reconstruct a surface from these discrete data. The most simple approach is to fit the data to a given algebraic surface with unknown parameters. The parameters describing the surface are obtained by the least squares solution.

We employed the conventional equation for aspheric surfaces with six high order coefficients.

$$z(\rho)=\frac{c\rho^2}{1+\sqrt{1-Qc^2\rho^2}}+\sum_{i=1}^{6}K_i\rho^{2i+2}. \quad (6)$$

where ρ is the radial coordinate, c is the vertex curvature, Q is the conic parameter, and K_i are the high order coefficients of the aspheric surface.

3. Examples of application of the design procedure

To show the potentials of the new design methodology I designed a set of positive and negative lenses. The lenses were assumed to be made of CR-39 plastic material ($n=1.498$). The lens diameter was set to 60 mm (diameter). The front aspheric surface was the designed one.

Four plus (1, 3, 5 and 7 D) and four negative lenses (−2.5, −5, −7.5 and −10 D) were designed. The vertex radius of curvature of the front surface was selected from typical base curve data extracted from the literature. Reference [4] provides (Tables 9.1 and 8.1 in [4]) the following typical base curve powers: 6, 7, 8, 11.5, 4, 4, 3 and 2 D for the 1, 3, 5, 7, −2.5, −5, −7.5 and −10 D lenses, respectively.

For plus lenses the central thickness is selected considering a required range of values for the edge thickness. We set the central thicknesses (Table 1) in order to provide an edge thickness close to 1 mm. Edge thickness increases with respect to the central thickness in negative lenses. So the central thickness is set as small as possible, taking into account mechanical stability. We selected a value of 1.6 mm [4] of central thickness for all the negative lenses.

The radius of curvature of the spherical posterior surface was finally calculated to provide the required lens power.

The surface profiles of the designed lenses are shown in Fig. 3, and the design parameters are given in Table 1. I observed that the optimal results were obtained if only the second derivatives where used for the least squares surface fitting.

3.1. Optical performance of the new designs

The optical performance of the new designs were evaluated by computing the tangential and sagittal power error as a function of gaze direction up to 40°. The results are plotted in Fig. 4 for the positive lenses and in Fig. 5 for the negative lenses. For comparative purposes these figures also show the tangential and sagittal power errors of spherical lenses with the radii of curvature matching that of the new aspheric lenses.

The tangential power error is virtually eliminated for all gaze directions (up to 40°) and for all the lenses (<0.1 D for all cases) in the new designs. The sagittal power errors are similarly in the new designs with respect to the spherical ones, though the values are significantly smaller for the negative lenses (with the exception of the −5 D lens). In general the optical improvement of the aspheric designs, with respect to spherical designs, is larger in the negative lenses. For example, for the −10 D lens the tangential power error is reduced from −0.32 D (spherical lens) to 0.07 D (aspheric) at 40°.

4. Conclusion

I have presented an efficient new procedure for optical design of single-vision aspheric lenses. The novelty of the procedure is that, rather than using conventional multi-parametric optimization, is based on point-by-point sequential surface construction. The algorithm, aim at eliminating tangential power error, is robust enough to virtually eliminate it up to 40° for positive and negative lenses.

Although the procedure has been developed to be used for rotationally symmetric lenses, it could be extended to astigmatic lenses. In that case the surface construction would be performed along with perpendicular meridians.

References

[1] D.A. Atchison, Optica Acta 32 (5) (1985) 607.
[2] M. Katz, Applied Optics 21 (1982) 2982.
[3] G. Esser, W. Becken, W. Mller, P. Baumbach, J. Arasa, D. Uttenweiler, Journal of the Optical Society of America. A 27 (2) (2010) 218.
[4] M. Jalie, Ophthalmic lenses and dispensing, Elsevier/Butterworth Heinemann, 2008.
[5] C. Fowler, K. Latham Petre, Spectacle lenses: theory and practice, Butterworth-Heinemann, 2001.
[6] G. Schulz, Optica Acta 32 (1985) 1361.
[7] W.S. Sun, C.L. Tien, C.C. Sun, M.W. Chang, H. Chang, Optical Engineering 39 (2000) 978.
[8] C.Y. Zhao, J.H. Burge, Journal of the Optical Society of America. A 19 (2002) 2313.
[9] C.Y. Zhao, J.H. Burge, Applied Optics 41 (2002) 7288.
[10] P. Benitez, J.C. Miano, J. Blen, R. Mohedano, J. Chaves, O. Dross, M. Hernandez, W. Falicoff, Optical Engineering 43 (7) (2004) 1489.
[11] J.B. Keller, H.B. Keller, Journal of the Optical Society of America. A 40 (1950) 48.
[12] J.A. Kneisly, Journal of the Optical Society of America. A 54 (1964) 229.
[13] J.E.A. Landgrave, J.R. MoyaCessa, Journal of the Optical Society of America. A 13 (8) (1996) 1637.
[14] C.E. Campbell, Journal of the Optical Society of America. A 23 (7) (2006) 1691.
[15] J.C. Chaves, Introduction to nonimaging optics, CRC Press, Boca Raton, 2008.
[16] E. Kreyszig, Differential geometry, Dover Publications, New York, 1991.